Am J Nucl Med Mol Imaging 2013;3(5):446-455
www.ajnmmi.us /ISSN:2160-8407/ajnmmi1308001

Original Article

Molecular MRI of atherosclerotic plaque progression in an ApoE$^{-/-}$ mouse model with a CLT1 peptide targeted macrocyclic Gd(III) chelate

Xueming Wu[1], Niranjan Balu[2], Wen Li[1], Yong Chen[1], Xiaoyue Shi[1], China M Kummitha[1], Xin Yu[1], Chun Yuan[2], Zheng-Rong Lu[1]

[1]*Department of Biomedical Engineering, Case Western Reserve University, Cleveland, OH 44106, USA;* [2]*Department of Radiology, University of Washington, Seattle, Washington 98019, USA*

Received August 8, 2013; Accepted September 2, 2013; Epub September 19, 2013; Published September 30, 2013

Abstract: Molecular imaging of atherosclerotic biomarkers is critical for non-invasive detection and diagnosis of atherosclerotic plaques and therapeutic management. Fibrin and fibronectin accumulate at elevated levels in atherosclerotic plaques and are associated with atherogenesis and disease progression. Molecular imaging of these biomarkers has the potential to non-invasively characterize plaque burden. In this work, we investigated the effectiveness of a peptide-targeted macrocyclic Gd(III) chelate, CLT1-dL-(DOTA-Gd)$_4$, specific to fibrin-fibronectin complexes for molecular MRI of atherosclerosis. Atherosclerotic plaques were induced in Apolipoprotein E-knockout (ApoE$^{-/-}$) mice by feeding with high fat and cholesterol-enriched diet (HFD) for up to 30 weeks. MRI of the vessel wall in the arch aorta was performed at 10, 20 and 30 weeks after the onset of HFD. High spatial-resolution MRI was performed prior and up to 35 minutes after i.v. injection of CLT1-dL-(DOTA-Gd)$_4$ or a nonspecific control agent at a dose of 0.1 mmol-Gd/kg. CLT1-dL-(DOTA-Gd)$_4$ produced stronger enhancement in the atherosclerotic lesions of the aortic wall than the control at all time points in the mice. Cross sectional MR images of the aortic arch revealed progressive thickening of the atherosclerotic vessel wall in the mice on HFD for up to 30 weeks. This progression correlated well to histological staining, as well as fibrin and fibronectin immunochemical stained images. Molecular MRI with CLT1-dL-(DOTA-Gd)$_4$ has a potential for detecting atherosclerosis and non-invasive monitoring of the progression of the plaques.

Keywords: Molecular MRI, atherosclerosis, CLT1 peptide, targeted contrast agent, macrocyclic Gd(III) chelate

Introduction

Atherosclerosis is a leading cause of cardiovascular morbidity and mortality worldwide [1]. The ability to non-invasively image atherosclerotic plaques and monitor disease progression is essential for reducing life-threatening cardiovascular events. Conventional clinical imaging modalities for atherosclerosis imaging are either invasive or unable to accurately assess the disease [2-5]. Noninvasive and high-resolution molecular imaging technologies are needed for more accurate characterization of atherosclerotic plaques and monitoring disease progression [6]. Molecular magnetic resonance imaging (MRI) is promising as a noninvasive imaging modality to detect and characterize atherosclerotic plaques because it lacks ionizing radiation and can measure molecular compositions of soft tissues with high spatial resolution [7, 8]. Targeted contrast agents are essential for MRI to measure the molecular compositions in the plaques and to detect pathological changes at the molecular level [9-12]. Current clinical contrast agents are non-specific to potential molecular targets of atherosclerosis and thus are not suitable for molecular MRI. The development of molecular MRI with safe and effective targeted contrast agents can address the clinical need for accurate detection and characterization of atherosclerotic plaques and non-invasive monitoring of disease progression.

Fibrin and Fibronectin are structural proteins that play a key role in the extracellular matrix

[13]. Numerous studies have shown that fibrin and fibronectin have high accumulation and form clots in the plaque tissues of human patients and ApoE$^{-/-}$ mice [14-20]. The elevated accumulation of fibrin and fibronectin in the arterial vessel wall contributes to the pathogenesis and progression of atherosclerosis [14-17]. It has been observed that fibrin(ogen) in thickened arterial intima promotes atherosclerosis and is associated with a poor clinical outcome [21]. The accumulation of fibronectin at atheroprone sites of the vessel wall increases endothelial permeability and inflammation by recruiting macrophages and consequently facilitates atherogenesis [18-20, 22]. Fibrin(ogen), fibronectin and their complexes are recognized as suitable biomarkers for non-invasive imaging and assessment of atherosclerotic plaques. Recent studies have demonstrated the feasibility of molecular MRI of intraplaque fibrin in ApoE$^{-/-}$ mice [12, 17]. The potential use of fibrin-fibronectin clots as a biomarker for molecular MRI of atherosclerosis and assessing plaque progression has not yet been explored with targeted Gd(III) based MRI contrast agents.

A cyclic decapeptide CLT1 (CGLIIQKNEC) was previously developed for specific binding to the fibrin-fibronectin clots accumulated in solid tumors and atherosclerotic plaques. The peptide showed specific binding to the clotted proteins in tumor with little binding to normal tissues [23-25]. We recently synthesized a small molecular CLT1 targeted macrocyclic Gd(III) chelate, CLT1-dL-(DOTA-Gd)$_4$, for molecular MRI of fibrin-fibronectin clots deposited in diseased tissues [25]. The agent produced significant contrast enhancement in the tumors with high accumulation of fibrin-fibronectin complexes. We hypothesized that CLT1-dL-(DOTA-Gd)$_4$ could also be effective for molecular MRI of the clotted plasma proteins in atherosclerotic plaques and for noninvasive monitoring of plaque progression. In this study, we investigated the effectiveness of the peptide targeted contrast agent for molecular MRI of fibrin-fibronectin clots in atherosclerotic plaques and monitoring the progression of atherosclerosis in ApoE$^{-/-}$ mice.

Materials and methods

MRI contrast agents

CLT1-dL-(DOTA-Gd)$_4$ was synthesized by conjugating four DOTA-Gd monoamide chelates to one CLT1 peptide [25]. A control agent with a scrambled CLT1 peptide (ClEGNKIQLC, sCLT1), sCLT1-dL-(DOTA-Gd)$_4$ was similarly synthesized by replacing the CLT1 with sCLT1. The contrast agents were purified by preparative HPLC for characterization and in vivo imaging experiment. The targeted contrast agent CLT1-dL-(DOTA-Gd)$_4$ has a molecular weight of 3,869 Da [25].

Animals

Homozygous B6.129P2-Apoe$^{tm1Unc/J}$ mice (ApoE$^{-/-}$) were purchased from Jackson laboratory (Bar Harbor, ME), and bred in the Animal Resource Center at Case Western Reserve University (CWRU). Animal housing and care were performed according to an animal protocol approved by the CWRU Institutional Animal Care and Use Committee. Mice were switched from normal diet to HFD (21% fat, 0.15% cholesterol, Harlan Laboratories, Madison, WI) when they were 8-weeks old for up to 30 weeks. The vital signs of mice, including body weight and skin infections, were monitored daily.

Fluorescence imaging

The targeting efficacy of CLT1 was verified with fluorescence imaging using a fluorescently labeled peptide, CLT1-Texas Red conjugate (CLT1-TR) [25]. CLT1-TR or sCLT1-Texas Red (sCLT1-TR) was intravenously injected to ApoE$^{-/-}$ mice on HFD for 10 weeks at a dose of 0.5 μmol/kg. One hour later, 100 IU/kg heparin was injected and allowed to circulate 10 min to prevent clot formation before euthanasia. The mice then were sacrificed and exsanguinated from the heart, perfused with ice-cold phosphate buffered saline (PBS, pH = 7.4) through the left ventricle to remove any unbound probes, and then the aorta was fixed by perfusion with 4% paraformaldehyde PBS. The whole aorta was dissected from the body and cut open longitudinally with a microscissor, pinned onto a black wax dissection pan and fixed with 4% paraformaldehyde overnight at 4°C. After removing connective tissue around the aorta, fluorescence imaging was taken on a Maestro instrument (Texas Red, Ex: Yellow, Em: 645 nm; software, yellow 10 nm steps (630:10:80)). After fluorescence imaging, the aorta was stained with Oil Red O to reveal the plaques.

MRI experiments

ApoE$^{-/-}$ mice on HFD were used to evaluate the efficacy of CLT1-dL-(DOTA-Gd)$_4$ with MRI. A

group of 6 mice was used for each agent at each time point. The MRI study was performed on a Bruker Biospec 9.4T MRI scanner (Bruker Corp., Billerica, MA, USA) with a volume radio frequency (RF) coil. Mice were anesthetized with a 2% isoflurane-oxygen mixture in an isoflurane induction chamber. A tail vein of each mouse was catheterized with a 30 gauge needle connected with a 2.5 m tubing filled with heparinized saline. The animal was then placed into the center of the volume RF coil and positioned in the magnet under continuous inhalation anesthesia with 1.5% isoflurane-oxygen via a nose cone. A respiratory sensor connected to a monitoring system (SA Instruments, Stony Brook, NY) was placed on the abdomen to monitor the rate and depth of respiration. The flow of anesthetic gas was constantly regulated to maintain a breathing rate of 50 ± 20 bpm. Body temperature was maintained at 35.0 ± 0.8°C by blowing hot air into the magnet through a feedback control system. ECG and respiratory gating was performed through an MR-compatible small animal gating and monitoring system (SA Instruments, Stony Brook, NY) to reduce motion artifacts during imaging. Heart rate was maintained at ~500 bpm with 0.8-1.8% isoflurane. A series of scout images were first acquired with a localizing sequence to identify the location of the heart. A 2D time-of-flight (TOF) angiogram (FOV = 2.92 × 2.92 cm^2; matrix = 200 × 200; slice thickness = 0.5 mm; repetition time (TR) = 15 ms; echo time (TE) = 3.5 ms; slices = 20; and flip angle = 60°) was then acquired axially. Based on the TOF maximum intensity projection images, high-resolution 2D black-blood MR images were planned in the oblique plane parallel to the aortic arch (IR-FLASH, FOV = 2.56 × 2.75 cm^2; TR = 88.8 ms; TE = 3.8 ms; slice thickness = 0.5 mm; interslice distance = 1.0 mm; echo = 1; slices = 4; average = 8; flip angle = 15°; matrix size = 256 × 256; inversion time = 30 ms). A subsequent high-resolution 2D T_1-weighted fast spin-echo black blood sequence with fat suppression (RARE factor 4, TR = 700 ms; TE = 9.7 ms; slice thickness = 0.5 mm; interslice distance = 0.5 mm; echo = 1; slices = 8; average = 10; flip angle = 90°; FOV = 2.92 × 2.92 cm^2; matrix size = 256 × 512; in-plane spatial resolution = 0.114 × 0.057 mm^2, inflow saturation band thickness = 30 mm with 2 mm section gap) was then acquired axially. The slices were positioned to cover the branch points of the carotid arteries, the ascending aorta, aortic arch, and proximal descending aorta. Contiguous cross-sectional images were obtained perpendicular to the long axis of the aorta. Baseline MR images were acquired before contrast. The agents were injected at a dose of 0.1 mmol-Gd/kg via the catheter. MR images were acquired at 5 and 35 min after the injection of CLT1-dL-$(DOTA\text{-}Gd)_4$ in mice at 10, 20 and 30 weeks on HFD and then with sCLT1-dL-$(DOTA\text{-}Gd)_4$ using the identical imaging parameters in the same group of mice one week later.

Histology and immunohistochemical studies

Some mice (n = 2) were sacrificed for histological studies immediately after the MRI experiment at 10 and 20 weeks, and all mice were sacrificed at 30 weeks. The aorta was excised using the same procedure as described for fluorescent imaging. The aorta was fixed and sectioned at locations closely corresponding to the axial MRI sections. Tissues were fixed with 4% paraformaldehyde and embedded in optimum cutting temperature (OCT) compound. Three consecutive tissue sections were selected for H&E staining, fibronectin staining, and fibrin staining, respectively. For fibrin and fibronectin staining, tissue sections with 5 μm thickness were fixed with pre-cooled fixative (acetone) for 5-10 min, and were incubated in 3% H_2O_2/MeOH for 30 minutes at room temperature to block endogenous peroxidase activity, incubated in 10% normal goat serum (NGS) in TBS for 30 min to block nonspecific binding. The sections were then incubated overnight at 4°C with primary antibodies at appropriate dilutions (rabbit polyclonal to fibronectin, mouse monoclonal (UC45) to fibrin alpha chain, Abcam). After washing with PBS, blocking with 10% NGS in TBS for 10 min, the secondary antibody (goat anti-rabbit IgG (H + L), horseradish peroxidase conjugate, Abcam) was applied for 30 min, and the signals were visualized using 0.75 mg/ml 3,3'-diaminobenzidine (DAB) with 0.015% hydrogen peroxide in Tris buffer. (DAB/DAB + Chromogen Solution, Dako).

Data analysis

MR image analysis was performed using Bruker ParaVision 4.0 imaging software. Regions of interest (ROIs) were drawn over the aortic wall and lumen of the axial MR images, and average signal intensity within the ROI was measured.

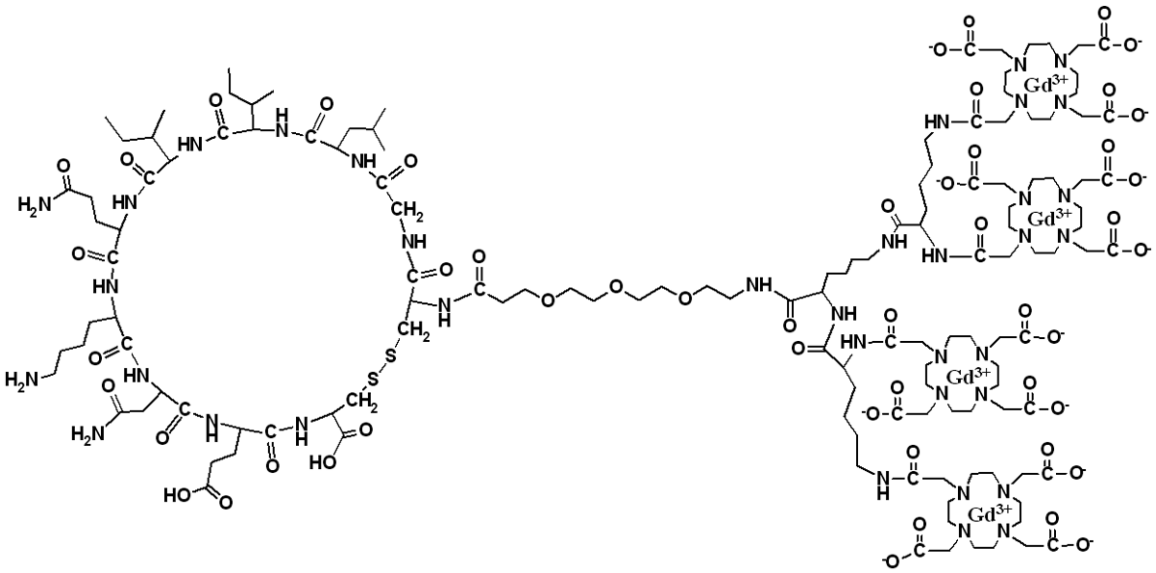

Figure 1. Structure of a peptide targeted MRI contrast agent CLT1-dL-(DOTA-Gd)$_4$.

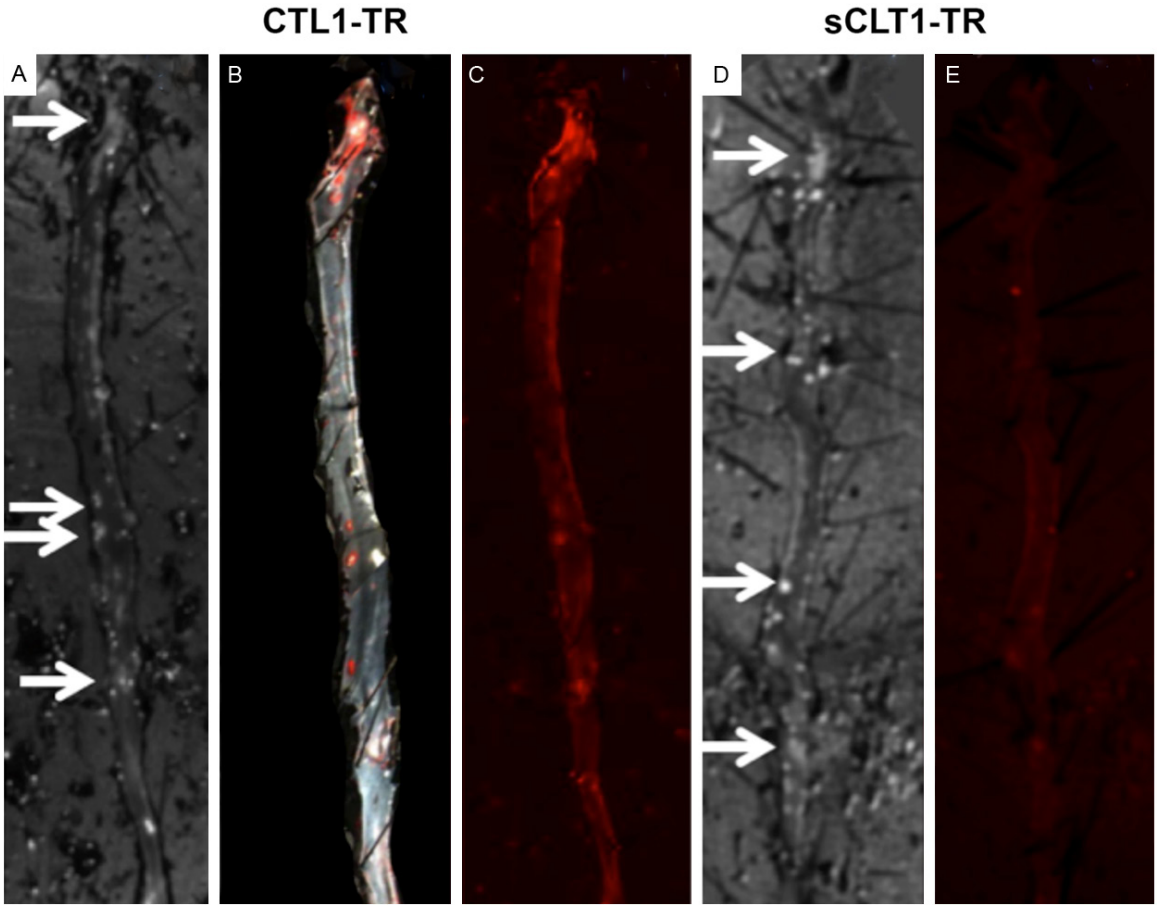

Figure 2. Ex vivo fluorescent imaging of the aortic tree from ApoE$^{-/-}$ mice 10 weeks on HFD. CLT1-TR and sCLT1-TR were injected intravenously with 0.5 μmol/kg and circulated for 1 h. The aorta was excised after perfusion and imaged ex vivo. A and D: Bright field; B: Oil Red O staining; C and E: TR fluorescence imaging. Arrows indicate the plaques.

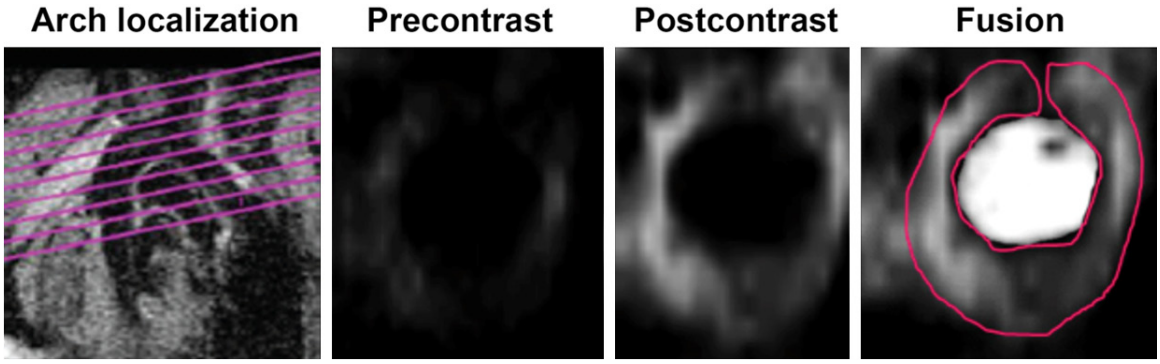

Figure 3. Cross-sectional views of the aortic arch artery of an ApoE$^{-/-}$ mouse 20-weeks on HFD. High-resolution axial MR images (pre and post contrast) were obtained by aligning the scans perpendicular to arch localization image (pink lines). Fusion of TOF and black-blood axial MRI provides spatial registration of contrast uptake and luminal anatomy.

Contrast to noise ratio (CNR) was calculated using the following equations: $CNR = (S_P-S_L)/\sigma$, where S_P and S_L denote the signal of the aortic wall and the lumen, σ is the standard deviation of noise. The *p* values were calculated using a student's two-tailed t-test, assuming statistical significance at $p < 0.05$.

Results

Targeted contrast agent

The structure of the targeted contrast agent CLT1-dL-(DOTA-Gd)$_4$ is shown in **Figure 1**. A generation 1 (G1) lysine dendrimer was used to increase the molar ratio of DOTA-Gd monoamide to the peptide in the agent for effective targeted contrast enhancement. The small size of the G1 lysine dendrimer would allow the unbound contrast agent to rapidly excrete from the body via renal filtration. The lysine dendrimer had a neutral core to minimize charge-associated non-specific tissue uptake. The peptide and lysine dendrimer were connected via a short PEG linker to avoid steric hindrance for target binding. sCLT1-dL-(DOTA-Gd)$_4$ with a scrambled peptide sCLT1 (CIEGNKIQLC) was used as non-targeted control agent. The r_1 relaxivity of free CLT1-dL-(DOTA-Gd)$_4$ and sCLT1-dL-(DOTA-Gd)$_4$ at 1.5 T and 37°C was 10.1 ± 1.0 and 11.5 ± 1.4 $mM^{-1}s^{-1}$ per Gd, respectively, which was about 3 times of that of DOTA-Gd (10.1 vs 2.9 $mM^{-1}s^{-1}$) [26].

CLT1 binding to atherosclerotic plaques in the aortic tree of mice

Figure 2 shows the bright field images and fluorescence images of the aortic tree from the mice on HFD for 10 weeks after injecting CLT1-TR or sCLT1-TR. The development of plaques in the aortic tree was confirmed by Oil Red O staining. As shown in **Figure 2B**, extensive plaques were formed at the branch points of the arch aorta, and some formed on the surface of the inner curvature of the ascending aorta. This observation was consistent with previous reports of plaque formation in ApoE$^{-/-}$ mice on high fat diet [10, 27]. Strong fluorescence signal of CLT1-TR was observed in the atherosclerotic plaque areas stained with Oil Red O, indicating the strong binding of the peptide probe in the atherosclerotic lesions. The non-specific scrambled probe sCLT1-TR resulted in little plaque binding. The co-localization of fluorescence signal from CLT1-TR and Oil Red O staining suggests that CLT1 peptide is effective for targeting atherosclerotic plaques.

Molecular MRI of atherosclerotic plaques with CLT1-dL-(DOTA-Gd)$_4$

The aortic arch was first localized using MR TOF angiography and high-resolution black blood MRI. High resolution axial MR images of the vessel wall of the carotid arteries, ascending aorta, aortic arch, and proximal descending aorta were then acquired using 2D T1-weighted black blood sequence with fat suppression. **Figure 3** shows the representative cross-sectional MR images of the aortic arch and the vessel wall images before and after injection of CLT1-dL-(DOTA-Gd)$_4$ of an ApoE$^{-/-}$ mouse 20-weeks on HFD. The targeted contrast agent resulted in strong enhancement in the atherosclerotic vessel wall. The contrast enhanced MR images reveal heterogeneous aortic wall

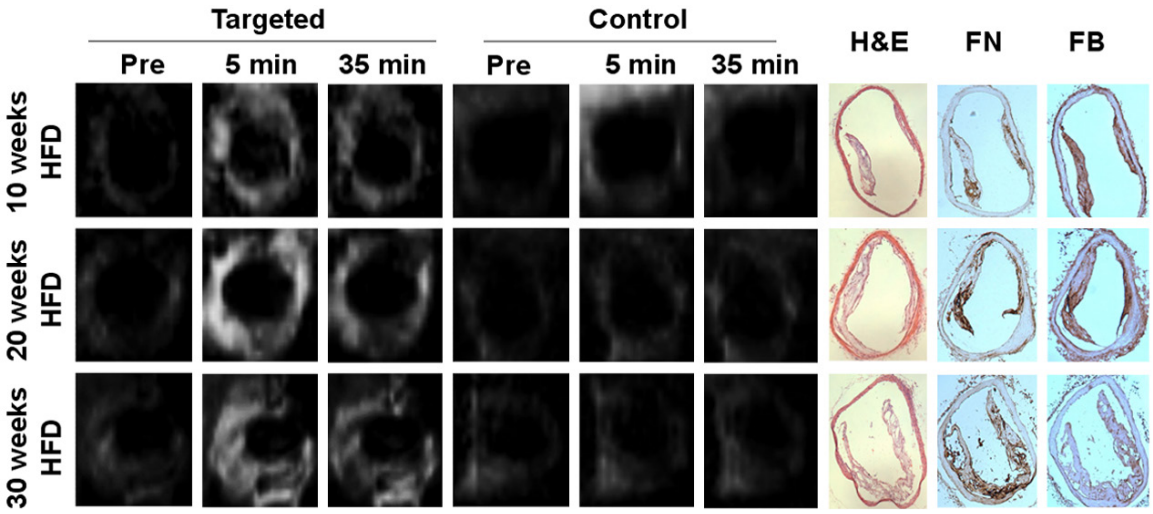

Figure 4. Cross-sections of MR images acquired in atherosclerotic ApoE$^{-/-}$ mice 10, 20 and 30 weeks after the onset of HFD at baseline (Pre, before injection), 5 and 35 min after injection of CLT1-dL-(DOTA-Gd)$_4$ and sCLT1-dL-(DOTA-Gd)$_4$ at a dose of 0.1 mmol Gd/kg. MR images with corresponding sections from H&E staining, fibronectin (FN) staining, and fibrin (FB) staining.

thickening, consistent with previous studies [10, 17].

Cross-section MR images of the aorta vessel wall of ApoE$^{-/-}$ mice were acquired at 10, 20 and 30 weeks on HFD first with the targeted agent CLT1-dL-(DOTA-Gd)$_4$ at a dose of 0.1 mmol-Gd/kg. One week later, after clearance of the targeted agent, MR images were then acquired with sCLT1-dL-(DOTA-Gd)$_4$. **Figure 4** shows the representative 2D axial T_1-weighted MR images of the atherosclerotic aorta wall acquired in ApoE$^{-/-}$ mice at 10, 20 and 30 weeks on HFD at baseline, 5 min, and 35 min after injection of CLT1-dL-(DOTA-Gd)$_4$ and sCLT1-dL-(DOTA-Gd)$_4$. Strong heterogeneous enhancement was observed in the aortic wall at all time points at 5 minutes after injection of CLT1-dL-(DOTA-Gd)$_4$, and little enhancement were observed for sCLT1-dL-(DOTA-Gd)$_4$. Although enhancement with the targeted agent decreased at 35 minutes after injection, it was still stronger than that from the control agent. The MR images also revealed progressive thickening of the atherosclerotic vessel wall in ApoE$^{-/-}$ mice on HFD.

Histochemical analysis revealed the formation of visible atherosclerotic plaques in ApoE$^{-/-}$ mice on HFD for 10 weeks and progressive wall thickening over time on HFD for up to 30 weeks. Immunohistochemical analysis using anti-fibrin and anti-fibronectin antibodies confirmed the presence of the clotted plasma proteins in the plaque (**Figure 4**). The MR images correlated well with the histochemical stains of the vessel wall and progressive vessel wall thickening. The result indicates that molecular MRI with CLT1-dL-(DOTA-Gd)$_4$ was effective to image the fibrin-fibronectin clots in atherosclerotic plaques and to monitor the disease progression.

Figure 5 shows the quantitative analysis of the contrast to noise ratio (CNR) of the MR images of the atherosclerotic vessel wall enhanced by CLT1-dL-(DOTA-Gd)$_4$ and sCLT1-dL-(DOTA-Gd)$_4$. The targeted agent CLT1-dL-(DOTA-Gd)$_4$ produced 140% and 91% CNR increase on average in the plaque tissue at 5 and 35 min after injection, respectively, in the mice at 10 weeks on HFD. By comparison, non-targeted sCLT1-dL-(DOTA-Gd)$_4$ only resulted in 74% and 42% increase in CNR. At 20 weeks on HFD, the targeted agent produced 144% and 77% CNR increase at 5 min and 35 min, while the non-targeted agent resulted in only 36% and 17% CNR increase, respectively. At 30 weeks on HFD, the targeted agent produced 62% and 59% CNR increase at 5 min and 35 min, while the non-targeted agent resulted in only 29% and 10% CNR increase, respectively. The targeted contrast agent produced more significant contrast enhancement in the plaques than the non-targeted control agent ($p < 0.05$), except at the 5 minute time point for the mice on HFD for 30 weeks. The CNR with both agents was lower at 5 minutes postinjection than other time

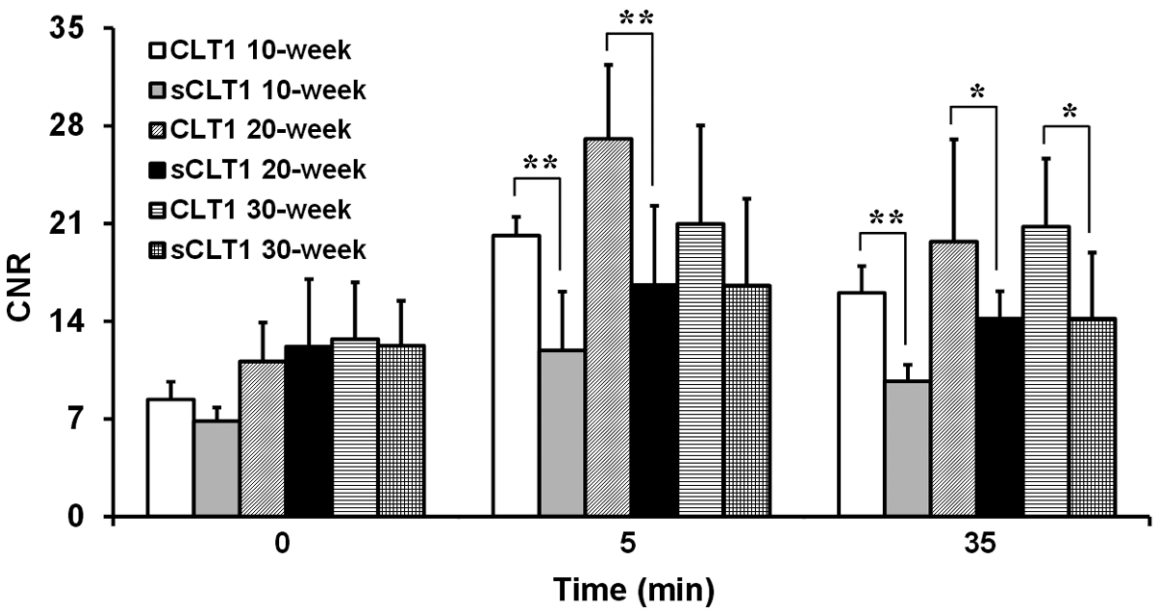

Figure 5. CNR in the plaques of the aortic wall before and at different time points after injection of CLT1-dL-(DOTA-Gd)$_4$ (CLT1) and sCLT1-dL-(DOTA-Gd)$_4$ (sCLT1) in ApoE$^{-/-}$ mice on HFD for 10, 20 and 30 weeks. *t*-test: $p < 0.01$ (**), $p < 0.05$ (*).

points possibly because of slow diffusion of the contrast agents in the thicker atherosclerotic vessel wall at 30 weeks on HFD. This could be the reason for the statistical insignificance ($p > 0.05$) of the CNR between the agents at 5 minutes after the injection at 30 weeks on HFD. Nevertheless, the targeted agent produced significantly higher CNR in the plaques at 35 minutes after the injection than the control agent ($p < 0.05$), when sufficient time was allowed for diffusion and washout of the agents.

Discussion

In the present study, we demonstrated the effectiveness of molecular MRI of fibrin-fibronectin clots deposited in atherosclerotic plaques using a small molecular peptide targeted macrocyclic Gd(III) chelate in a mouse model of atherosclerosis model. It is challenging for contrast enhanced MRI to visualize disease related biomarkers with a small molecular targeted contrast agent due to its poor sensitivity. Due to the abundance of fibrin and fibronectin in atherosclerotic plaques verified by immunohistochemical analysis, a sufficient amount of CLT1-dL-(DOTA-Gd)$_4$ was able to bind to plasma protein clots accumulated in the atherosclerotic plaques and to produce robust contrast enhancement for effective molecular MRI. Molecular MRI with CLT1-dL-(DOTA-Gd)$_4$ was also effective for monitoring plaque progression. Previous investigations showed that prominent presence of fibrin and fibronectin were associated with the progression of atherosclerosis [16, 17, 20]. Histochemical analysis in this study showed the growth of the atherosclerotic lesions in the aortic arch from 10 to 30 weeks on HFD and strong presence of both fibrin and fibronectin in the lesions. The contrast enhanced MR images of the atherosclerotic vessel wall correlated well with histochemical and immunohistochemical analyses. The contrast enhanced MR images with the targeted contrast agent clearly showed the size increase of the atherosclerotic lesions from 10 to 30 weeks on HFD. These results suggest that the targeted agent can be useful for determining the progression of atherosclerosis.

The pathological roles of fibrin and fibronectin in atherosclerosis formation and progression have been discussed in numerous reports [12-22]. Fibrin is generally associated with the inflamed endothelium and the necrotic core of plaques, and has a high accumulation in the luminal thrombus [16, 21]. Fibronectin is also associated with inflammation and recruitment of macrophages in atherosclerotic plaques [18-20, 22]. Fibronectin accumulates in the extra-

cellular matrix of plaques by complexing with fibrin or collagen in the tissue. Fibrin has been investigated as a molecular target for MRI of luminal thrombosis [28-31]. It has been recently reported that the fibrin is also a potential molecular target for molecular MRI of atherosclerotic plaques in ApoE$^{-/-}$ mice on HFD [12, 17]. We have shown in this study that fibrin-fibronectin clots are a promising target for molecular MRI of atherosclerosis.

The main concern for clinical development of any new Gd(III) based MRI contrast agents is safety. It is known that nephrogenic systemic fibrosis is associated with Gd(III) based MRI contrast agents, especially linear Gd(III) chelates, in patients with compromised renal function. Linear Gd(III) chelates, Gd-DTPA and derivatives, suffer from poor kinetic inertness and can release toxic Gd(III) ions due to transmetallation with endogenous metal ions, such as Zn^{2+}. Macrocyclic Gd(III) chelates, such as the DOTA-Gd derivative used in this study, generally have a high kinetic inertness against transmetallation [33, 34]. Four DOTA-Gd monoamide chelates were conjugated to each peptide to improve the targeted enhancement efficiency of the peptide. The overall r_1 relaxivity of CLT1-dL-(DOTA-Gd)$_4$ was 40 $mM^{-1}s^{-1}$/molecule, over 10 time greater than DOTA-Gd [26]. High overall relaxivity allowed the agent to produce strong enhancement at a relatively low dose (0.1 mmol-Gd/kg). The agent also had a relatively low molecular weight, which allowed the unbound agent to be readily cleared from the blood circulation. In previous work, it was shown that the blood pool half-life of the agent was approximately 2 minutes [25]. Rapid clearance of the agent from blood circulation decreased background noise in the blood and surrounding tissues and allowed for rapid excretion of the agent through renal filtration. The biodistribution study showed that the agent had low tissue accumulation 48 hours after injection [25]. High kinetic inertness and rapid clearance of the agent are crucial for minimizing the potential toxic side effects.

There are several limitations in the current study. We noticed that CLT1-dL-(DOTA-Gd)$_4$ washed out relative quickly from the targeting site in the first five minutes post-injection, especially in the mice with relatively small plaques. In vivo proteolytic degradation might cause the degradation of CLT1 peptide and the loss of binding ability of the contrast agent. Modification of CLT1 peptide may prevent proteolytic degradation, improve its stability and prolong binding and contrast enhancement. Replacement of some of the L-amino acids in CLT1 peptide with corresponding D-amino acids could be an effective strategy to achieve this goal. Additionally, the MRI study was performed on a high-field MRI animal scanner (9.4 T). T_1-weighted contrast enhanced MRI with Gd(III) based contrast agent at the high field strength is not as effective as at the field strength range of commonly used clinical scanners (1.5 and 3 T) because of long T_1 relaxation time of water protons and reduced relaxivity of the contrast agents at high field strengths. It is expected that the targeted contrast agent will be more effective for molecular MRI of atherosclerosis at 1.5 or 3 T than the high field strength used in this study. Although fibrin and fibronectin clots are present in both human and ApoE$^{-/-}$ mouse atherosclerotic lesions, the mouse atherosclerosis model is not the optimal model for evaluating the ability of the targeted agent to characterize plaque stability. Future studies will be focused on increasing the in vivo peptide stability by structural modification and a comprehensive determination of the pharmacokinetics, biodistribution, retention and safety of the targeted contrast agent for translational development.

Conclusion

The peptide targeted macrocyclic Gd(III) chelate CLT1-dL-(DOTA-Gd)$_4$ effectively produced significant contrast enhancement in atherosclerotic plaques in ApoE$^{-/-}$ mice on HFD. Molecular MRI revealed the progressive thickening of the atherosclerotic vessel wall of the arch aorta, which correlated well to histological staining of plaques and immunohistochemical staining of fibrin and fibronectin. Molecular MRI with CLT1-dL-(DOTA-Gd)$_4$ was effective for noninvasively imaging atherosclerosis and monitoring the progression of the plaque lesions. This agent has a potential to noninvasively detect and characterize atherosclerotic plaques.

Acknowledgements

The work is funded in part by the American Heart Association GRA Spring 09 Postdoctoral Fellowship (09POST2250268) and the NIH R01 EB00489.

Disclosure of conflict of interest

None.

Address correspondence to: Dr. Zheng-Rong Lu, Department of Biomedical Engineering, Case Western Reserve University, Room 427, Wickenden Building, 10900 Euclid Avenue, Cleveland, OH 44106-7207, USA. Tel: 216-368-0187; E-mail: zxl125@case.edu

References

[1] Roger VL, Go AS, Lloyd-Jones DM, Benjamin EJ, Berry JD, Borden WB, Bravata DM, Dai S, Ford ES, Fox CS, Fullerton HJ, Gillespie C, Hailpern SM, Heit JA, Howard VJ, Kissela BM, Kittner SJ, Lackland DT, Lichtman JH, Lisabeth LD, Makuc DM, Marcus GM, Marelli A, Matchar DB, Moy CS, Mozaffarian D, Mussolino ME, Nichol G, Paynter NP, Soliman EZ, Sorlie PD, Sotoodehnia N, Turan TN, Virani SS, Wong ND, Woo D and Turner MB. Heart disease and stroke statistics-2012 update: a report from the american heart association. Circulation 2012; 125: e2-e220.

[2] Kwan AC, Cater G, Vargas J and Bluemke DA. Beyond coronary stenosis: coronary computed tomographic angiography for the assessment of atherosclerotic plaque burden. Curr Cardiovasc Imaging Rep 2013; 6: 89-101.

[3] Madaj P and Budoff MJ. Risk stratification of non-contrast CT beyond the coronary calcium scan. J Cardiovasc Comput Tomogr 2012; 6: 301-307.

[4] Kawasaki M, Sano K, Okubo M, Yokoyama H, Ito Y, Murata I, Tsuchiya K, Minatoguchi S, Zhou X, Fujita H and Fujiwara H. Volumetric quantitative analysis of tissue characteristics of coronary plaques after statin therapy using three-dimensional integrated backscatter intravascular ultrasound. J Am Coll Cardiol 2005; 45: 1946-1953.

[5] Jang IK, Bouma BE, Kang DH, Park SJ, Park SW, Seung KB, Choi KB, Shishkov M, Schlendorf K, Pomerantsev E, Houser SL, Aretz HT and Tearney GJ. Visualization of coronary atherosclerotic plaques in patients using optical coherence tomography: comparison with intravascular ultrasound. J Am Coll Cardiol 2002; 39: 604-609.

[6] Waxman S, Ishibashi F and Muller JE. Detection and treatment of vulnerable plaques and vulnerable patients: novel approaches to prevention of coronary events. Circulation 2006; 114: 2390-2411.

[7] Briley-Saebo KC, Mulder WJM, Mani V, Hyafil F, Amirbekian V, Aguinaldo JGS, Fisher EA and Fayad ZA. Magnetic resonance imaging of vulnerable atherosclerotic plaques: Current imaging strategies and molecular imaging probes. J Magn Reson Imaging 2007; 26: 460-479.

[8] Corti R and Fuster V. Imaging of atherosclerosis: magnetic resonance imaging. Eur Heart J 2011; 32: 1709-1719.

[9] Chen W, Cormode DP, Vengrenyuk Y, Herranz B, Feig JE, Klink A, Mulder WJM, Fisher EA and Fayad ZA. Collagen-specific peptide conjugated HDL nanoparticles as MRI contrast agent to evaluate compositional changes in atherosclerotic plaque regression. JACC Cardiovascular Imaging 2013; 6: 373-384.

[10] Makowski MR, Wiethoff AJ, Blume U, Cuello F, Warley A, Jansen CHP, Nagel E, Razavi R, Onthank DC, Cesati RR, Marber MS, Schaeffter T, Smith A, Robinson SP and Botnar RM. Assessment of atherosclerotic plaque burden with an elastin-specific magnetic resonance contrast agent. Nat Med 2011; 17: 383-388.

[11] Amirbekian V, Aguinaldo JGS, Amirbekian S, Hyafil F, Vucic E, Sirol M, Weinreb DB, Le Greneur S, Lancelot E, Corot C, Fisher EA, Galis ZS and Fayad ZA. Atherosclerosis and matrix metalloproteinases: experimental molecular MR imaging in vivo. Radiology 2009; 251: 429-438.

[12] Flacke S, Fischer S, Scott MJ, Fuhrhop RJ, Allen JS, McLean M, Winter P, Sicard GA, Gaffney PJ, Wickline SA and Lanza GM. Novel MRI contrast agent for molecular imaging of fibrin implications for detecting vulnerable plaques. Circulation 2001; 104: 1280-1285.

[13] Pereira M, Rybarczyk BJ, Odrljin TM, Hocking DC, Sottile J and Simpson-Haidaris PJ. The incorporation of fibrinogen into extracellular matrix is dependent on active assembly of a fibronectin matrix. J Cell Sci 2002; 115: 609-617.

[14] Loeffen R, Spronk HM and Cate H. The impact of blood coagulability on atherosclerosis and cardiovascular disease. J Thromb Haemos 2012; 10: 1207-1216.

[15] Stępien E, Kabłak-Ziembicka A, Musiałek P, Tyłko G and Przewłocki T. Fibrinogen and carotid intima media thickness determine fibrin density in different atherosclerosis extents. Int J Cardiol 2012; 157: 411-413.

[16] Tavora F, Cresswell N, Li L, Ripple M and Burke A. Immunolocalisation of fibrin in coronary atherosclerosis: implications for necrotic core development. Pathology 2010; 42: 15-22.

[17] Makowski MR, Forbes SC, Blume U, Warley A, Jansen CH, Schuster A, Wiethoff AJ and Botnar RM. In vivo assessment of intraplaque and endothelial fibrin in ApoE(-/-) mice by molecular MRI. Atherosclerosis 2012; 222: 43-49.

[18] Stenman S, von Smitten K and Vaheri A. Fibronectin and atherosclerosis. Acta Med Scand Suppl 1980; 642: 165-170.

[19] Smith EB and Ashall C. Fibronectin distribution in human aortic intima and atherosclerotic lesions: concentration of soluble and collagenase-releasable fractions. Biochim Biophys Acta 1986; 880: 10-15.
[20] Moore KJ and Fisher EA. The double-edged sword of fibronectin in atherosclerosis. EMBO Mol Med 2012; 4: 561-563.
[21] Undas A, Nowakowski T, Cieśla-Dul M and Sadowski J. Abnormal plasma fibrin clot characteristics are associated with worse clinical outcome in patients with peripheral arterial disease and thromboangiitis obliterans. Atherosclerosis 2011; 215: 481-486.
[22] Feaver RE, Gelfand BD, Wang C, Schwartz MA and Blackman BR. Atheroprone hemodynamics regulate fibronectin deposition to create positive feedback that sustains endothelial inflammation. Circ Res 2010; 106: 1703-1711.
[23] Pilch J, Brown DM, Komatsu M, Jarvinen TA, Yang M, Peters D, Hoffman RM and Ruoslahti E. Peptides selected for binding to clotted plasma accumulate in tumor stroma and wounds. Proc Natl Acad Sci U S A 2006; 103: 2800-2804.
[24] Ye F, Wu X, Jeong EK, Jia Z, Yang T, Parker D and Lu ZR. A peptide targeted contrast agent specific to fibrin-fibronectin complexes for cancer molecular imaging with MRI. Bioconjug Chem 2008; 19: 2300-2303.
[25] Wu X, Burden-Gulley SM, Yu GP, Tan M, Lindner D, Brady-Kalnay SM and Lu ZR. Synthesis and evaluation of a peptide targeted small molecular Gd-DOTA monoamide conjugate for MR molecular imaging of prostate cancer. Bioconjug Chem 2012; 23: 1548-1556.
[26] Rohrer M, Bauer H, Mintorovitch J, Requardt M and Weinmann HJ. Comparison of magnetic properties of MRI contrast media solutions at different magnetic field strengths. Invest Radiol 2005; 40: 715-724.
[27] Maeda N, Johnson L, Kim S, Hagaman J, Friedman M and Reddick R. Anatomical differences and atherosclerosis in apolipoprotein E-deficient mice with 129/SvEv and C57BL/6. Atherosclerosis 2007; 195: 75-82.
[28] Yu X, Song SK, Chen JJ, Scott MJ, Fuhrhop RJ, Hall CS, Gaffney PJ, Wickline SA and Lanza GM. High-resolution MRI characterization of human thrombus using a novel fibrin-targeted paramagnetic nanoparticle contrast agent. Magn Reson Med 2000; 44: 867-872.
[29] Botnar RM, Buecker A, Wiethoff AJ, Parsons EC, Katoh M, Katsimaglis G, Weisskoff RM, Lauffer RB, Graham PB, Gunther RW, Manning WJ and Spuentrup E. In vivo magnetic resonance imaging of coronary thrombosis using a fibrin-binding molecular magnetic resonance contrast agent. Circulation 2004; 110: 1463-1466.
[30] Sirol M, Aguinaldo JGS, Graham PB, Weisskoff R, Lauffer R, Mizsei G, Chereshnev I, Fallon JT, Reis E, Fuster V, Toussaint JF and Fayad ZA. Fibrin-targeted contrast agent for improvement of in vivo acute thrombus detection with magnetic resonance imaging. Atherosclerosis 2005; 182: 79-85.
[31] Overoye-Chan K, Koerner S, Looby RJ, Kolodziej AF, Zech SG, Deng Q, Chasse JM, McMurry T and Caravan P. EP-2104R: A fibrin-specific gadolinium-based MRI contrast agent for detection of thrombus. J Am Chem Soc 2008; 130: 6025-6039.
[32] White GW, Gibby WA and Tweedle MF. Comparison of Gd(DTPA-BMA) (Omniscan) versus Gd(HP-DO3A) (ProHance) relative to gadolinium retention in human bone tissue by inductively coupled plasma mass spectroscopy. Invest Radiol 2006; 41: 272-278.
[33] Wu X, Zong Y, Ye Z and Lu ZR. Stability and biodistribution of a biodegradable macromolecular MRI contrast agent Gd-DTPA cystamine copolymers (GDCC) in rats. Pharm Res 2010; 27: 1390-1397.
[34] Ye Z, Wu X, Tan M, Jesberger J, Griswold M and Lu ZR. Synthesis and evaluation of a polydisulfide with Gd–DOTA monoamide side chains as a biodegradable macromolecular contrast agent for MR blood pool imaging. Contrast Media Mol Imaging 2013; 8: 220-8.